Cryogenics 60 (2014) xxx–xxx

Contents lists available at ScienceDirect

Cryogenics

journal homepage: www.elsevier.com/locate/cryogenics

Emissivity of silver and stainless steel from 80 K to 300 K: Application to ITER thermal shields

S.I. Woods [a,*], T.M. Jung [b], D.R. Sears [b], J. Yu [c]

[a] National Institute of Standards and Technology, 100 Bureau Drive, Gaithersburg, MD 20899, United States
[b] Jung Research and Development Corp., 1706 U St. NW #204, Washington, DC 20009, United States
[c] ITER Organization, Route de Vinon-sur-Verdon, 13115 St. Paul-lez-Durance, France

ARTICLE INFO

Article history:
Received 3 September 2013
Received in revised form 28 December 2013
Accepted 9 January 2014
Available online 21 January 2014

Keywords:
Cryogenic emissivity
Thermal shields
Emissivity of silver coatings
Radiation thermometry
Absolute cryogenic radiometer

ABSTRACT

The emissivities of thermal shield mock-up samples for ITER have been measured at sample temperatures between 80 K and 300 K using an optical method employing a primary standard broadband detector. These thermal shields, made from SS304L stainless steel coated with silver, are designed to operate at 80 K, protecting the superconducting magnet system of the ITER reactor from higher temperature regions. Our results show that the silver coating of the thermal shields can have an emissivity as low as 0.0035 at 80 K, approximately ten times lower than the emissivity of the bare polished stainless steel plate. We demonstrate that the emissivity of different regions of a thermal shield assembly can be determined in a single measurement cycle, providing further emissivity data on the insulating spacer used to separate shield plates as well as emissivity data on a silver coating repair method. The temperature dependence of the emissivity for the silver coating agrees well with a theoretical estimate based on the Drude model including phonon and surface-assisted scattering.

Published by Elsevier Ltd.

1. Introduction

The thermal shields for the International Thermonuclear Experimental Reactor (ITER) will protect the reactor's superconducting magnet system, which must be maintained at 4.5 K, from warmer regions. The vast majority of cooling for the entire reactor will be provided by cooling water, but these shields for the magnet system will be cooled by 80 K flowing helium gas, and the load on the superconducting magnets will be minimized by using a low emissivity coating for the thermal shield plates. Silver coatings have been used and tested in previous fusion reactor designs [1,2], and a new set of silver-coated thermal shield mock-up samples have been designed and fabricated for ITER [3].

Knowledge about the low temperature emissivity of materials and coatings can be essential to the design of fusion cryoplants and in the thermal modeling for space satellite missions [4,5]. The emittance of thermal shields, light baffles, and other components at operational temperatures often cannot be predicted from room temperature data, but for computing radiative loads and infrared backgrounds this cryogenic data is often required. Previous emissivity measurements on silver coatings have often had poorly documented, potentially large uncertainties and lacked enough data to elucidate the temperature dependence of emissivity from 80 K to 300 K. Particularly at cryogenic temperatures, there has been significant variation in the emissivity determined for silver coatings, either as a result of sample variation or measurement error [2,6,7].

Measurements of the cryogenic emissivity of a highly reflective surface such as silver is a significant challenge: little thermal power is radiated from the sample, and the background radiation, even within an enclosed cryogenic vacuum chamber, can be stronger than the signal if the background radiators have higher emissivity than the sample. Furthermore, for the lowest sample temperatures required in this measurement, nearly all of the signal is at wavelengths beyond 20 μm so detection into the far-infrared is imperative. We have developed an optical method using an absolute cryogenic radiometer (ACR) primary standard with high responsivity to 200 μm and beyond which can be used to characterize the emissivity of samples at setpoint temperatures between 80 K and 300 K [8]. Measurements are made in a high-vacuum cryogenic chamber which provides a low background radiation environment, and samples with cross-sections up to 400 mm × 400 mm can be accommodated. Uncertainty in the measurement is minimized by background subtraction using a cooled shutter and by careful estimation of the reflected signal from the sample, as well as the estimation of the emitted and reflected signals from the cooled shutter.

We have made emissivity measurements on three thermal shield mock-up samples, all of which were made from stainless

* Corresponding author. Tel.: +1 (301) 975 2382.
E-mail address: solomon.woods@nist.gov (S.I. Woods).

http://dx.doi.org/10.1016/j.cryogenics.2014.01.002
0011-2275/Published by Elsevier Ltd.

steel plates with various surface treatments and coatings. Emissivity was determined for a bare polished stainless steel plate, for a plate with a pristine silver coating, and for a damaged silver coating which had been fixed using a repair method. Two of the samples were simple plates with welded cooling tubes, and one sample was an assembly consisting of two stainless steel plates with welded cooling tubes, an insulating spacer (G-10), and a cavity region. On the more complicated thermal shield assembly, we demonstrated that the emissivity for each of several distinct regions of a sample can be determined during a single measurement cycle.

At 80 K, the emissivity of the undamaged silver coating was found to be 0.0035 with a standard uncertainty of 0.00033 (coverage factor $k = 1$), less than one-tenth of the emissivity of the bare stainless steel plate. For both the stainless steel and silver coating, the emissivity is approximately linear as a function of temperature from 80 K to 300 K. The emissivity for the silver coating exhibits reasonable agreement with an analytical expression for the normal emissivity of a good conductor developed by Sievers et al. from a model which includes phonon and surface-assisted scattering in the Drude approximation [9,10]. Compared to the undamaged silver coating, the repaired silver coating displays an emissivity approximately 20–40% higher over the range from 80 K to 300 K. Results for the thermal shield assembly with insulating spacer show that even though the G-10 spacer only accounts for 0.5% of the assembly area, it produces nearly 50% of the thermal emission at 80 K because the emissivity of the insulator is nearly unity.

2. Experimental details

Three somewhat different mock-up samples allowed comparison of the emissivities of stainless steel, a pristine silver coating, a damaged and repaired silver coating, and allowed analysis of a thermal shield assembly including an insulating spacer. Sample A is a 300 mm × 300 mm plate made from polished SS304L stainless steel approximately 10 mm thick, with two stainless steel cooling tubes welded to one side of the plate, as shown in Fig. 1. The roughness of the polished surface is at most 0.3 μm. Sample B started as a plate identical to Sample A, but in a final step it was electroplated with a layer of silver at least 5 μm thick. Sample C is an assembly made from two SS304L stainless steel plates, separated by a thin spacer of fiberglass–epoxy laminate (G-10), and bolted together. The full assembly is approximately 400 mm × 300 mm, with thickness between 20 mm and 56 mm, as shown in Fig. 2. The geometry of the plates defines a small inner cavity and there are two stainless steel cooling tubes welded to one side of each plate. The roughness of the stainless steel surfaces before silver plating was at most 0.3 μm. Then the plates were assembled with the insulating spacer and the silver surface was damaged with scratches. In a second coating step, a repair layer of silver was deposited by a selective electrochemical metallization (SEM) method over the damaged electroplated coating.

The measurement method has been described in detail in an earlier paper [8] but, in brief, we have utilized a radiation thermometry technique with background subtraction employing an absolute cryogenic radiometer (ACR) as the detector. All emissivity measurements were conducted within a helium-gas cooled cryogenic vacuum chamber with diameter approximately 0.6 m and length 3 m, which contained both the sample enclosure and detector. The base temperature of the chamber shrouds was approximately 25 K, and the detector was mounted to a liquid helium cryostat within the vacuum chamber at 2 K. The sample could be independently cooled by helium gas flowed through its cooling tubes to a minimum temperature of 20 K or heated by resistive heaters to a maximum temperature of 300 K. The ACR is a primary standard detector with an absorptivity estimated to be 99.93% in the mid-infrared, around 99% at 100 μm, and greater than 97% at 200 μm. A cold shutter between the sample and detector was used to make background measurements, and very low temperature measurements of the sample were used to quantify power from the shutter and any power offset of our measurement system.

As presented in Ref. [8], the background-subtracted power measured at a setpoint temperature $T_s = T_{set}$ is given by:

$$(S_s - S_{sh})^{(meas)}_{|T_s=T_{set}} = [\varepsilon_s \Gamma T_s^4 \mathcal{D}_s - \varepsilon_s \Gamma \varepsilon_b T_b^4 \mathcal{D}_b - \varepsilon_{sh} \Gamma T_{sh}^4 \mathcal{D}_{sh} + \varepsilon_{sh} \Gamma \varepsilon_b T_b^4 \mathcal{D}_b]_{|T_s=T_{set}} \quad (1)$$

where Γ is a power-scaled configuration factor and T_α, ε_α and $\mathcal{D}_\alpha$ ($\alpha \in \{s, sh, b\}$) are the temperature, emissivity and diffraction factor for the sample (s), shutter (sh) and background (b). The diffraction factor accounts for the effects of diffraction on the optical throughput of the system, and it is equal to the ratio between the expected power at the detector including diffraction effects and the expected power at the detector considering only geometrical optics. The emissivity of the sample is then calculated from the ACR measurements using the expression:

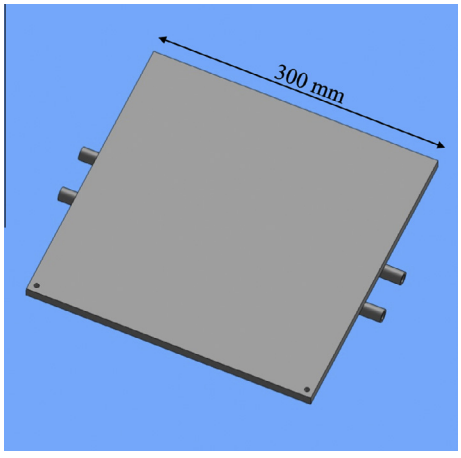

Fig. 1. Schematic of Sample A, a plate of polished SS304L stainless steel with two stainless steel cooling tubes welded to one side. Sample B is identical to Sample A in geometry and composition, except that it is additionally coated with a thin layer of silver.

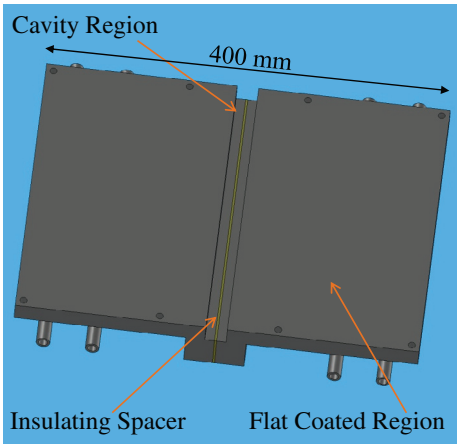

Fig. 2. Schematic of Sample C, an assembly made from two silver-coated SS304L stainless steel plates, separated by a thin spacer of fiberglass–epoxy laminate (G-10), and bolted together.

$$\varepsilon_{s|T_s=T_{set}} = \left(\frac{(S_s - S_{sh})^{(meas)}}{\mathcal{D}_s}_{|T_s=T_{set}} - \frac{(S_s - S_{sh})^{(meas)}}{\mathcal{D}_{sh}}_{|T_s=T_{base}} \right) \Big/ (\Gamma T_s^4)_{|T_s=T_{set}} + \left(\left[\varepsilon_{sh} T_{sh}^4 \frac{\mathcal{D}_{sh}}{\mathcal{D}_s} - (\varepsilon_{sh} - \varepsilon_s^{(0)}) \varepsilon_b T_b^4 \frac{\mathcal{D}_b}{\mathcal{D}_s} \right]_{|T_s=T_{set}} + \left[\varepsilon_s^{(0)} T_s^4 \frac{\mathcal{D}_s}{\mathcal{D}_{sh}} - \varepsilon_{sh} T_{sh}^4 + (\varepsilon_{sh} - \varepsilon_s^{(0)}) \varepsilon_b T_b^4 \frac{\mathcal{D}_b}{\mathcal{D}_{sh}} \right]_{|T_s=T_{base}} \right) \Big/ (T_s^4)_{|T_s=T_{set}} \quad (2)$$

where the first two terms on the right-hand side are from the ACR measurements and the other terms are composed of measured temperatures and measured or tabulated emissivities. The notation "$|T_s = T_{set}$" or "$|T_s = T_{base}$" indicates that the relevant terms are measured or calculated for the sample at a setpoint temperature T_{set} (various temperatures between 80 K and 300 K) or at the sample base temperature T_{base} (typically 20 K). Measurements made with the sample plate at the base temperature allow for the quantification and subtraction of small power offsets related to leakage radiation from the sample enclosure or to differences in the background-scene dependent on the shutter position. The $\varepsilon_s^{(0)}$ term is a first order estimate of sample emissivity given by just the first two terms on the right-hand side of Eq. (2), neglecting the shutter and background correction terms. Given that the measurement optical train has an *f*-number greater than 10, the emissivity thus calculated is a directional broadband emissivity, at approximately the normal to the sample source. Using an aperture near the sample plate, the view of the detector is limited to the central 102 mm diameter region of the sample.

3. Measurement results

Sample A and Sample B allow a direct comparison of the emissivity of polished SS304L stainless steel plate and the silver coating because both samples are nominally the same except Sample B is coated with greater than 5 μm of silver in a final fabrication step. Emissivity as a function of sample setpoint temperature is plotted for both Sample A and Sample B in Fig. 3. The standard uncertainty in the emissivity for each sample is indicated by error bars in the figure. Uncertainty for each parameter of Eq. (2) was determined from repeated measurements (Type A uncertainty) or by estimation (Type B uncertainty) and these uncertainties were propagated using Eq. (2) to determine the combined uncertainty in the emissivity [8]. Table 1 displays values of emissivity and its standard uncertainty at temperatures between 80 K and 300 K for polished SS304L stainless steel (Sample A) and for a silver coating (Sample B). Table 2 is an itemized list detailing the contributions to the total emissivity uncertainty from each of the parameters in Eq. (2) for the measurement of Sample B. Over the ranges probed in the experiment, these parameters are assumed to be independent.

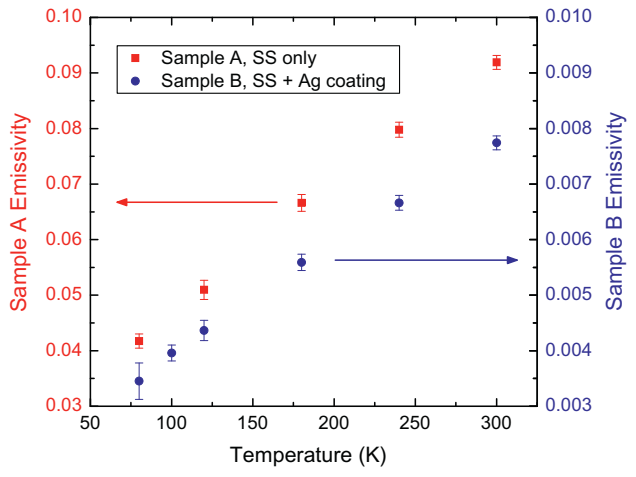

Fig. 3. Emissivity as a function of temperature for Sample A and Sample B, with error bars ($k = 1$) indicated. The silver coating lowers the emissivity by more than a factor of 10 compared to the bare polished SS304L stainless steel surface.

Table 1
Tabulated values of emissivity and its standard uncertainty at temperatures between 80 K and 300 K for polished SS304L stainless steel (Sample A) and for a silver coating (Sample B).

Temperature (K)	SS304L stainless steel		Silver	
	Emissivity	Uncertainty ($k = 1$)	Emissivity	Uncertainty ($k = 1$)
80	0.0417	0.0013	0.00350	0.00033
100			0.00399	0.00014
120	0.0510	0.0017	0.00439	0.00018
180	0.0666	0.0015	0.00561	0.00015
240	0.0798	0.0014	0.00667	0.00013
300	0.0919	0.0013	0.00775	0.00013

Table 2
Uncertainty contributions ($k = 1$) from various experimental parameters to the calculated emissivity for Sample B, at setpoint temperature 80 K. For each parameter in the list other than the power-scaled configuration factor Γ, the uncertainty represents a combination of the uncertainties at the setpoint temperature (T_{set} = 80 K) and the base temperature (T_{base} = 20 K).

Experimental parameter	Contribution to emissivity uncertainty	Relative contribution to variance (%)
$(S_s - S_{sh})^{(meas)}$	7.27×10^{-5}	4.89
T_s	1.42×10^{-4}	18.66
T_{sh}	9.61×10^{-5}	8.54
T_b	2.41×10^{-4}	53.63
ε_{sh}	9.05×10^{-6}	0.08
ε_b	2.53×10^{-5}	0.59
$\varepsilon_s^{(0)}$	1.19×10^{-4}	13.11
$\mathcal{D}_s$	1.10×10^{-6}	<0.01
$\mathcal{D}_{sh}$	2.04×10^{-5}	0.38
$\mathcal{D}_b$	6.14×10^{-6}	0.03
Γ	8.92×10^{-6}	0.07
Total	3.29×10^{-4}	100

Sample C, a thermal shield assembly comprised of two silver-coated stainless steel plates and an insulating G-10 spacer, allows measurements of the emissivity of the repaired silver coating as well as an investigation of the relative contributions of the plates and insulating spacer at various temperatures from 80 K to 300 K. During measurements, three different areas of Sample C were exposed by rotating the cooled shutter to three different locations. In the first shutter position all sample regions (insulating spacer, cavity, flat plate) were exposed, in the second position only the cavity and flat regions were exposed, and in the third position only flat plate was exposed. Using emissivity data calculated at each of these shutter positions and data on the dimensions of the thermal shield assembly, the emissivity of each separate region of Sample C (insulating spacer, cavity, flat plate) could be separately calculated [8]. The emissivity from 80 K to 300 K for the insulating spacer (G-10) and flat plate (silver coating) regions of the sample, with standard uncertainties indicated by error bars, are shown in Fig. 4. The ratio of the emissivity of the flat region of Sample C (ε_C) to the emissivity of Sample B (ε_B) is plotted in Fig. 5.

4. Analysis of results and discussion

For the stainless steel plate and silver coatings measured, the emissivity is approximately linear in temperature between 80 K

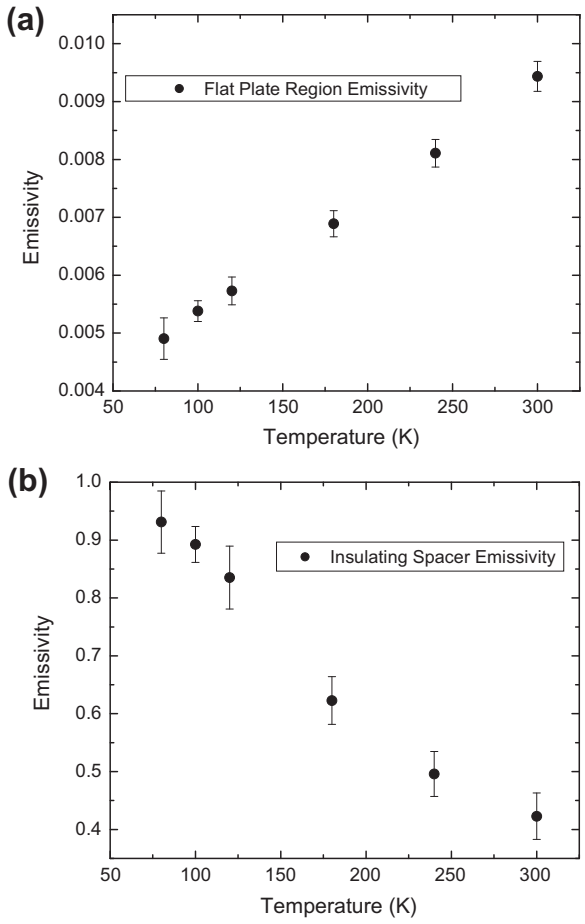

Fig. 4. Emissivity as a function of temperature for (a) the flat part (silver coating) of Sample C and (b) the insulating spacer (G-10) of Sample C, with error bars ($k = 1$) indicated.

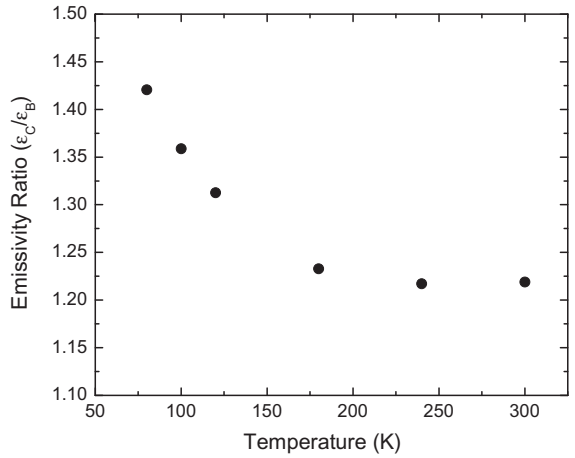

Fig. 5. Ratio of the emissivity of the flat region of Sample C (ε_C) to the emissivity of Sample B (ε_B). This ratio provides a comparison of the emissivity of a repaired silver coating with an undamaged silver coating. The repaired coating exhibits an emissivity excess of approximately 40% at 80 K and 20% at 300 K.

and 300 K, as seen in Figs. 3 and 4. For a thermally-emitting sample, this temperature dependence is consistent with an emissivity which is independent of wavelength and proportional to resistivity. The emissivity of a good conductor such as silver has been investigated theoretically and can be approximated in the extreme relaxation region ($\omega\tau \gg 1$) by the Mott-Zener result $\varepsilon = 2/\omega_p\tau$, where ω_p is the plasma frequency and τ is the electron relaxation time. Sievers and co-workers have developed approximate expressions for the relaxation time in a model including electron–phonon and electron-surface scattering in the Drude approximation [9,10], and our data exhibits reasonable agreement with their estimates. Fig. 6 presents the normal emissivity from the silver coatings of Sample B and Sample C, as well as the theoretical estimate for bulk silver from Sievers et al. Also presented in Fig. 6 are experimental results from Ramanathan et al. for the emissivity of silver at temperatures from 400 K to 540 K using a calorimetric method [11]. The Ramanathan et al. results were presented as hemispherical emissivity data, so these results have been multiplied by 0.75 to approximate normal resistivity, since it has been determined that for good conductors the ratio of normal to hemispherical resistivity is approximately 0.75 [9].

Unlike the metallic materials, the emissivity of the G-10 fiberglass–epoxy laminate in Sample C is maximal at the lowest temperatures and falls to about 40% near room temperature, as can be seen in Fig. 4b. This behavior is consistent with the emissivity of glasses which usually displays an infrared cutoff resulting from a "forest" of phonon excitations in the infrared [12,13]. At temperatures well below room temperature, nearly all the thermal radiation is emitted at wavelengths beyond 20 μm, where glasses are generally fully-absorbing. At the temperatures near room temperature, a significant fraction of the thermal radiation is emitted at wavelengths shorter than 10 μm where it appears that the fiberglass–epoxy laminate is at least somewhat transmitting. The cavity region of Sample C exhibits somewhat enhanced emissivity from the flat part of the plate, due in part to the cavity effect (reflections within the cavity) and in part to reflections of radiation emitted by the insulating G-10 spacer.

The individual emissivity data for each of the regions of Sample C allows an understanding of the relative contributions of each region to the overall assembly emittance and of the temperature dependence of the full assembly emittance. Fig. 5 shows that the repaired silver coating has an excess emissivity of approximately 41% at 80 K and excess emissivity of approximately 22% at 300 K when compared with the undamaged coating. By considering the relative areas of insulating spacer, cavity and flat plate in the assembly, the relative contribution from each of the sample regions to the emittance of the full assembly can be calculated from the emissivity results extracted for each region. The relative contribution of each region to the total emittance as a function of set-point temperature is displayed in Fig. 7. In Fig. 7, it can be seen that at 80 K the insulating G-10 spacer is a significant contributor

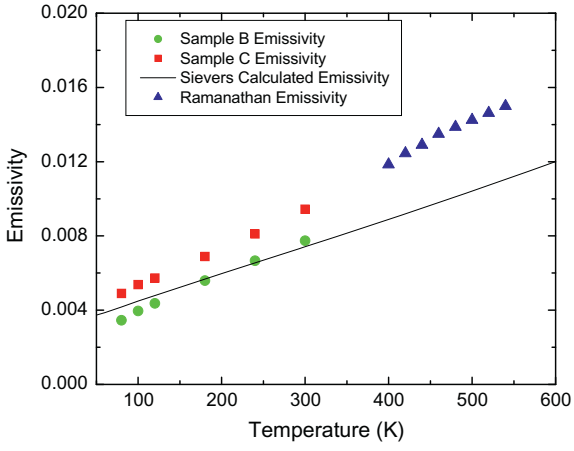

Fig. 6. Comparison of silver emissivity measured in this work with previous theoretical (Sievers, Ref. [9]) and experimental (Ramanathan, Ref. [11]) studies.

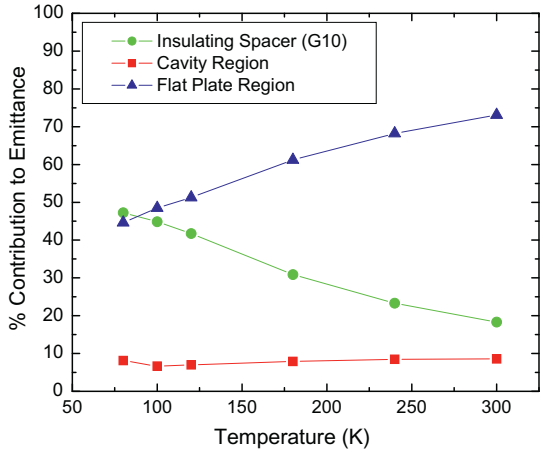

Fig. 7. Relative contributions of each region of Sample C to the emittance of the entire assembly, as a function of temperature. At 80 K, the thin insulating spacer accounts for over 47% of the emittance, even though it only accounts for about 0.5% of the assembly surface area.

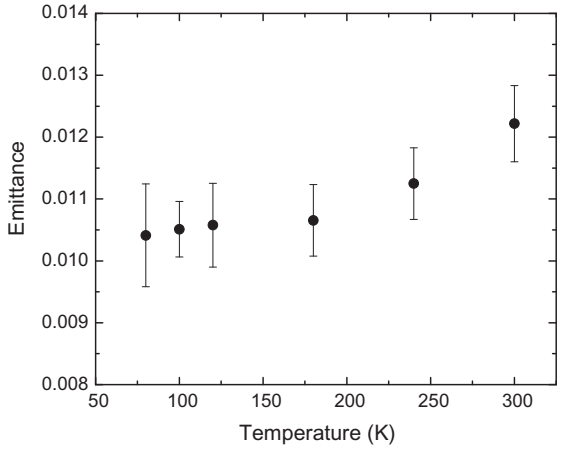

Fig. 8. Emittance as a function of temperature for the entire Sample C assembly, with error bars ($k = 1$) indicated.

to the measurement emittance. Even though the insulating spacer accounts for only about 0.5% of the area of the assembly, its emissivity is nearly 200 times higher than that of the silver coating, so its emittance contribution is approximately equal to that of the remainder of the assembly. The normal emittance of the entire Sample C assembly in the far field, calculated from the emissivities in Fig. 4 and the relative areas of the different regions, is plotted in Fig. 8 over the temperature range from 80 K to 300 K. The Sample C emittance is near 0.01 and fairly flat as a function of temperature. The contribution of the flat coated region rises linearly with temperature, but the emissivity of the insulating spacer falls quickly with temperature, so these changes partially cancel to yield only a weak temperature dependence for the emittance of the full assembly.

5. Conclusions

The silver coating significantly reduces the emissivity of the thermal shield plate compared to the bare polished SS304L stainless steel surface at all temperatures from 80 K to 300 K. The undamaged silver coating at 80 K exhibits an emissivity of 0.0035, less than one-tenth of the emissivity of the bare polished stainless steel plate. Even the silver coating with repair exhibits an emissivity less than 0.005 at the shield operating temperature of 80 K. Results on Sample C show that the insulating G-10 spacer, with an emissivity near unity at low temperatures, can contribute significantly to the emittance of the entire plate at 80 K. It could be worthwhile to metallize the exposed surface of the insulating spacer in order to reduce the contribution of this region to thermal emittance.

Apparent emissivity from the thermal shields can vary as a function of position and potentially time. One useful follow-on experiment could be to measure emissivity at different sample-detector angles and separation distances. Another potentially useful experiment would be to measure the emissivity of the silver-coated thermal shields as the silver coating ages and tarnishes.

References

[1] Lipa M, Martinez A, Lacroix B, Chatain D. Experience with silver coated vacuum vessel thermal shield at 80 K in Tore Supra. In: 2009 23RD IEEE/NPSS symposium on fusion engineering; 2009. p. 603–6.
[2] Ageladarakis PA, Obert W. On the emissivity of silver coated panels, effect of long term stability and effect of coating thickness. In: DewHughes D, Scurlock RG, Watson JHP, editors. International cryogenic engineering conference 1998; 1998. p. 715–8.
[3] Noh CH, Nam K, Chung W, Kang DK, Kim BC, Utin Y, et al. Manufacture and test of mock-up for ITER thermal shield. Fusion Eng Des 2010;85:1880–4.
[4] Herve P, Rambure N, Sadou A, Ramel D, Francou L, Delouard P, et al. Direct measurement of total emissivities at cryogenic temperatures: application to satellite coatings. Cryogenics 2008;48:463–8.
[5] Tolson W, Or C, Glazer S, Kobel M, Packard E. Determination of coating emittance at cryogenic temperatures for the James Webb Space Telescope – experimental methods and results. In: JB Heaney, LG Burriesci, editors. Cryogenic optical systems and instruments XI. Proceedings of SPIE, vol. 5904; 2005. p. 59040G.
[6] Duckworth RC, Demko JA, Gouge MJ, Urbahn JA. Measurement of the emissivity of clean and contaminated silver plated copper surfaces at cryogenic temperatures. In: Balachandran U, editor. Advances in cryogenic engineering, vol. 52; 2006. p. 61–68.
[7] Dickson PF, Jones MC. Infrared reflectances of metals at cryogenic temperatures—a compilation from the literature. NBS Tech Note 1966;348:1–60.
[8] Woods SI, Jung TM, Ly GT, Yu J. Broadband emissivity calibration of highly reflective samples at cryogenic temperatures. Metrologia 2012;49:737–44.
[9] Sievers AJ. Thermal radiation from metal surfaces. J Opt Soc Am 1978;68(11):1505–16.
[10] Smalley R, Sievers AJ. The total hemispherical emissivity of copper. J Opt Soc Am 1978;68(11):1516–8.
[11] Ramanathan KG, Yen SH. High-temperature emissivities of copper, aluminum and silver. J Opt Soc Am 1977;67(1):32–8.
[12] Beattie JR, Coen E. Spectral emission of radiation by glass. Br J Appl Phys 1960;11:151–7.
[13] Isard JO. Surface reflectivity of strongly absorbing media and calculation of the infrared emissivity of glasses. Infrared Phys 1979;20:249–56.